GHGT-11

CO$_2$ pipeline integrity: A coupled fluid-structure model using a reference equation of state for CO$_2$

E. Aursand[a], P. Aursand[a], T. Berstad[c], C. Dørum[b], M. Hammer[a],
S. T. Munkejord[a]* and H. O. Nordhagen[b]

[a] SINTEF Energy Research, P.O. Box 4671 Sluppen, NO-7465 Trondheim, Norway
[b] SINTEF Materials and Chemistry, P.O. Box 4670 Sluppen, NO-7465 Trondheim, Norway
[c] Norwegian University of Science and Technology (NTNU), Dept. of Structural Engineering, NO-7491 Trondheim, Norway

Abstract

We present a coupled fluid-structure model to study crack propagation and crack arrest in pipelines. Numerical calculations of crack arrest, crack velocity and pressure profiles have been performed for steel pipes with an outer diameter of 267 mm and a wall thickness of 6 mm. The pipe material and fracture propagation have been modelled using the finite-element method with a local ductile fracture criterion and an explicit time-integration scheme. An in-house finite-volume method has been employed to simulate the fluid dynamics inside the pipe, and the resulting pressure profile was for each time step applied as a load in the finite-element model. Choked-flow theory was used for calculating the flow through the pipe opening as the crack propagated. Simulations were performed with both methane and CO$_2$, pressurized at 75, 120 and 150 bar. Initial results indicate that crack arrest does not necessarily occur with CO$_2$ under circumstances where it would occur with methane.

1. Introduction

For the deployment of CO$_2$ capture and storage (CCS), transport between the sites of capture and those of storage will be required. If CCS is to attain the significant scale needed [1, Tab. 15.1], large pipeline networks will be involved, entailing several research challenges. Today, onshore CO$_2$ pipelines exist and are operated for the purpose of enhanced oil or gas recovery and are mainly situated in remote areas.

* Corresponding author. Tel.: +47 73 59 38 97; fax: +47 73 59 28 89.
E-mail address: svend.t.munkejord@sintef.no.

However, future CCS pipelines will to a larger extent pass through or near densely populated areas. This will impose restrictions regarding health, safety and environment (HSE), including pipeline integrity. Furthermore, for economic reasons, it is desirable to reduce oversizing and the use of expensive material qualities. This calls for validated and physically based tools for the evaluation of CO_2 pipeline integrity, including the avoidance of long running fractures.

A running fracture in a pipeline could be initiated by corrosion or third-party damage. If the fluid pressure inside the pipe causes sufficient crack driving forces, the crack will propagate rapidly along the pipeline. At the same time, the opening of the pipe will cause a depressurization of the fluid inside. Therefore, this is a coupled fluid-structure problem, and it should be modelled as such. A key challenge involves modelling of what we term the *fracture race*: The depressurization of the fluid inside the pipeline is governed by the pressure-propagation velocity (speed of sound), which is significantly slower in the two-phase region than in the single-phase region. As long as the crack-driving forces cause a load on the propagating crack that exceeds the fracture resistance of the pipe, the crack will continue to propagate. Further, if the pressure-propagation velocity is slower than the crack-propagation velocity, the pressure at the crack tip will remain high and sufficient for sustaining a stable high crack velocity – and the crack will continue to propagate. Otherwise, if the pressure-propagation velocity is faster than the crack-propagation velocity, and the crack driving forces are decreasing, the crack will at some point arrest by itself.

It should be noted that evaluation methodologies for running ductile fracture commonly employed today (such as the Battelle [2] and HLP methods [3]) are empirically based and not primarily developed for CO_2 or modern ductile steels. These models assume the behaviour of the fluid and the structure during fracture propagation to be uncoupled processes, and were developed for pipeline material qualities used 30–40 years ago for transport of natural gas. Moreover, they require cumbersome re-calibration when changing the pressurized fluid inside the pipe, or when new material qualities are introduced. The trend seen today is to use pipelines with higher strength and toughness, as well as lower pipe wall thicknesses. There are strong indications that the empirical basis developed earlier does not apply for these new conditions (e.g. [4]).

In the present work, we model both the pipeline itself and the fluid flow inside the pipe and through the crack in a physically reasonable, yet computationally tractable, way. The flow inside the pipe is modelled as one-dimensional single-, two- or three-phase flow. The resulting model is solved in a robust and accurate way using the multistage centred (MUSTA) method [5,6]. The flow through the crack is assumed to be fast and therefore adiabatic and quasi steady state. The pipeline material is modelled using shell elements and an elasto-viscoplastic material model and the fracture is modelled using a local ductile fracture model with element erosion. The structural pipeline model is implemented in the finite-element (FE) code LS-DYNA [7] with explicit time stepping.

The fluid and structure models are fully coupled. At every time-step, the pipeline model supplies the crack opening profile to the fluid model. Using this information, the fluid model calculates the leakage rate and hence the axial pressure distribution, which in the next timestep is used as a load to the structural pipeline model, determining the crack width, etc.

The present method is an extension of the one described and experimentally validated by Nordhagen *et al.* [8,9] for the single-phase flow of hydrogen and methane. Here, the thermodynamic properties and phase equilibria of CO_2 are accounted for using the reference equation of state (EOS) by Span and Wagner [10]. The flow model also handles the formation of three phases, including dry ice.

The rest of this paper is organized as follows. Section 2 and 3 present the details of the structural model and the fluid model, respectively, while Section 4 explains how the two are coupled. In Section 5, calculations of crack propagation in a pipeline filled with methane and CO_2 are performed. Section 6 concludes the paper and suggests topics for further work.

2. The pipeline model

This section presents the constitutive models and the adopted ductile fracture criterion for modelling the mechanical properties of the steel pipeline material. In this work, an API 5L-X65mod ERWpipe material, with an outer diameter of 267 mm and a wall thickness of 6 mm is investigated. It is well known that pipe materials have a certain degree of anisotropic plastic behaviour as a result of the manufacturing process [11,12]. However, in this work we have used an isotropic yield function (von-Mises).

The yield function f, which defines the elastic domain in stress space, is expressed in the form

$$f(\boldsymbol{\sigma}, R) = \bar{f}(\boldsymbol{\sigma}) - (Y_0 + R) \leq 0 , \tag{1}$$

where Y_0 is the reference yield stress, and R is the isotropic work-hardening variable. In Eq. (1) $\bar{\sigma} = \bar{f}(\boldsymbol{\sigma})$ is the effective stress and $\sigma_y = Y_0 + R$ is the flow stress, representing the strength of the material. The flow stress is defined by the non-linear isotropic hardening rule

$$\sigma_Y = \sigma_0 + \sum_{i=1}^{2} Q_i (1 - \exp(-C_i \varepsilon_e)) , \tag{2}$$

where σ_0 is the proportionality limit, ε_e is the equivalent plastic strain, and Q_i and C_i are hardening parameters. The hardening parameters in Eq. (2) were calibrated by using data from uniaxial tensile tests from specimens oriented in the circumferential direction of the pipe, giving: $\sigma_0 = 521.8$ MPa, $Q_1 = 183.5$ MPa, $Q_2 = 3655$ MPa, $C_1 = 39.1$, $C_2 = 77.3$. The triaxial stress state encountered in the neck of the circular specimen was taken into account when calibrating the uniaxial hardening curve. Crack propagation is described by element erosion when a fracture criterion is fulfilled within the element:

$$W = \int \max(\sigma_1, 0) d\varepsilon_e \leq W_c , \tag{3}$$

where σ_1 is the maximum principal stress, and W_c is the value of the Cockcroft-Latham integral, W, giving fracture. This criterion implies that fracture is a function of the integrated tensile (principal) stress σ_1 and equivalent plastic strain ε_e, and has the dimensions of work per unit volume. In the present study, the fracture parameter was identified from uniaxial tension tests: $W_c = 1200$ MPa. Based on the material constitutive equations (1)–(3), the non-linear FE equations, and the loading conditions supplied by the fluid code and the external boundary conditions, the displacement of the nodes in the structure and the resulting stresses and strains are calculated in LS-DYNA through an explicit integration scheme.

3. The flow model

This section briefly describes the employed models for the flow in the pipe and the flow through the crack. The description is based on [9], but we highlight the new elements arising from the inclusion of multi-phase flow of CO_2.

3.1. Governing equations

In this work, the single-phase flow through a pipe is modelled as one-dimensional and inviscid,

$$\frac{\partial \rho}{\partial t} + \frac{\partial (\rho u)}{\partial x} \quad = \quad -\varsigma_e ,$$

$$\frac{\partial (\rho u)}{\partial t} + \frac{\partial (\rho u^2)}{\partial x} + \frac{\partial p}{\partial x} \quad = \quad -u \varsigma_e , \qquad (4)$$

$$\frac{\partial E}{\partial t} + \frac{\partial \left[(E + p)u \right]}{\partial x} \quad = \quad -(E_e + p_e) \frac{1}{\rho_e} \varsigma_e ,$$

where x is position, t is time, and ρ, p and u are the density, pressure and the velocity in x direction, respectively. The total volumetric energy of the fluid can be written $E = \rho(e + u^2/2)$, where e is the internal specific energy. Here it is assumed that in multi-phase flow, there is no slip between the phases. Therefore, the formulation (4) is retained, but with ρ and E as mixture quantities, e.g. $\rho = (\alpha \rho)_g + (\alpha \rho)_l + (\alpha \rho)_s$ and $E = (\alpha \rho)_g (e + u^2/2)_g + (\alpha \rho)_l (e + u^2/2)_l + (\alpha \rho)_s (e + u^2/2)_s$, where α is the volume fraction and subscript g, l and s denote gas, liquid and solid.

The right-hand side of (4) represents the leakage of the fluid through a crack in the pipeline. The subscript e indicates that the quantity in question is evaluated at the escape point in the crack. The source-term factor ς_e represents the mass loss due to the leakage, and it is given by

$$\zeta_e = \rho_e u_e \frac{2r_e}{A} , \qquad (5)$$

where $2r_e(x)$ is the crack opening width at position x, and A is the cross-sectional area of the pipe, see Figure 1.
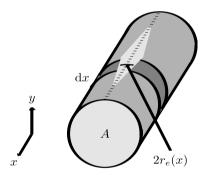

Figure 1: The crack propagates along the x-direction, leaving behind a growing opening of width $2r_e(x)$ in the pipe.

Ahead of the crack tip, it is reasonable to assume the flow to be 1D, but this assumption does not necessarily hold behind the crack tip. However, the added source term can effectively account for the y-directed escape flow due to the initial leakage of the fluid through the crack opening. As the opening widens, the 1D character of the fluid flow will naturally degenerate, but this is believed to be less important with respect to the crack driving forces (e.g. [13,14]).

With a suitable equation of state (EOS), the escape quantities can be expressed as functions of the state of the fluid within the pipe, as well as of the crack opening width and the surrounding pressure. There are three escape quantities which need to be calculated: u_e, p_e and ρ_e. The crack width $2r_e$ is supplied by the pipeline model described in Section 2. The specific internal energy e_e is not needed since Bernoulli's principle for isentropic flow states that the stagnation enthalpy is constant along a flow line. The first part of the third source term in (4) may then be written as

$$\frac{E_e + p_e}{\rho_e} = h_e + \frac{u_e^2}{2} = h_i + \frac{u_i^2}{2} \, , \tag{6}$$

showing that initial quantities (subscript *i*) from inside the pipe may be used instead of calculating e_e.

3.1.1. Methane
For single-phase flow of gases well above their critical point, the ideal gas EOS

$$p = (\gamma - 1)e\rho \, , \tag{7}$$

where $\gamma = c_p/c_v$ is the ratio of the specific heats, works sufficiently well. Initially, when the inside-to-outside pressure ratio is larger than or equal to $[(\gamma + 1)/2]^{\gamma/(\gamma-1)}$, the flow velocity will attain the speed of sound, i.e., the flow is choked. If one assumes that the escape flow is an isentropic process, the following expressions hold:

$$\rho_e = \rho \left(\frac{2}{\gamma + 1} \right)^{1/(\gamma-1)} \, , \tag{8}$$

$$u_e = a_e = a\sqrt{\frac{2}{\gamma + 1}} \, , \tag{9}$$

where *a* is the speed of sound. When the inside-to-outside pressure ratio falls below the choked flow criterion, it is still possible to derive the corresponding expressions,

$$\rho_e = \left(\frac{p_a}{p} \right)^{1/\gamma} \rho \, , \tag{10}$$

$$u_e = a\left\{ \frac{2}{\gamma - 1}\left[1 - \left(\frac{p_a}{p} \right)^{(\gamma-1)/\gamma} \right] \right\}^{1/2} \, . \tag{11}$$

For an on-shore pipeline, the surrounding pressure p_a usually corresponds to the atmospheric pressure, and that has been assumed in the following calculations.

3.1.2. Carbon dioxide
In the case of CO_2, the ideal gas EOS (7) is replaced with the Span–Wagner [10] reference equation of state. The employed numerical method is explained and discussed by Giljarhus *et al.* [15]. To include dry-ice, the model is extended using the Span–Wagner auxiliary function for sublimation pressure, and a simple temperature polynomial for the dry-ice density,

$$\rho_{solid}(T) = A \cdot T^2 + B \cdot T + C \, , \tag{12}$$

where A=−0.0224 kg/(m^{3}K^2), B=6.8896 kg/(m^{3}K) and C=1070.8 kg/m^3.

The entropy of dry-ice, s_{solid}, in equilibrium with gas can then be described using the Clapeyron equation,

$$\frac{dP}{dT} = \frac{s_{gas} - s_{solid}}{1/\rho_{gas} - 1/\rho_{solid}} \, . \tag{13}$$

For the flow through the crack, the choked-flow relations of the previous paragraphs cannot be employed, due to the more complex form of the EOS, and due to the possibility of phase change during the decompression. Here, we employ an isentropic homogeneous equilibrium choke model, in which Bernoulli's equation is written for a streamline going through the crack. This gives the following choke condition

$$\frac{1}{2}\left(a_e^2 - u_i^2\right) + \int_{p_i}^{p_e} \frac{\mathrm{d}p'}{\rho(p', s)} = 0 \ , \tag{14}$$

where u_i is the initial velocity of the streamline, while p_i and p_e denote the pressures inside the pipe and at the escape point, respectively. The entropy s is constant along the streamline. By assuming that one may set $u_i = 0$, one may show that satisfying the above choke condition is equivalent to finding a pressure between the initial and ambient which maximizes the mass flux through the escape point, *i.e.*

$$p_e = \left\{ p \in [p_i, p_a] : \frac{\mathrm{d}}{\mathrm{d}p}\left(\rho(p)^2 \int_{p_i}^{p} \frac{\mathrm{d}p'}{\rho(p')} \right) = 0 \right\} \ . \tag{15}$$

The integral is evaluated by constructing a Newton interpolation polynomial for $\rho(p)$ at the given entropy, to limit the number of calls to the Span–Wagner EOS. If such a maximizing pressure is found, the escape flow is choked, and the escape pressure is equal to (15). If a maximizing pressure cannot be found, the flow must be non-choked, and the escape pressure is equal to the ambient pressure. In both cases the escape velocity is given by Bernoulli's equation (with $u_i = 0$):

$$u_e = \sqrt{-2\int_{p_i}^{p_e} \frac{\mathrm{d}p'}{\rho(p')}} \tag{16}$$

3.2. Numerical solution

The governing equations (4) are discretized using the Finite-Volume method. They are then solved numerically employing the multi-stage centred (MUSTA) scheme by Toro and coworkers [5,6]. Details are omitted here for brevity. The MUSTA scheme has been investigated and found to be robust and accurate for different two-phase flow models, including drift-flux [16,17] and two-fluid [18] models.

4. The fluid-structure coupling scheme

This section briefly explains how the fluid model is coupled to the structural pipeline model. For more detailed information on the coupling scheme and the burst tests used to verify the methane simulations, see [9] and references therein. The coupled fluid-structure problem was modelled using the structure models of Section 2 implemented in the LS-DYNA [7] code, and the thermo and fluid dynamics models of Section 3 implemented in an in-house code. The coupling scheme involves the following steps, where steps 3–6 are run in a continuous cycle until the crack stops propagating (arrests):

1) Pipeline pressure set to operational pressure. This is done quasi-statically in LS-DYNA. The initial pressure is used in the initialization of the fluid code.
2) Erosion of elements corresponding to the length of the initial damage caused on the pipe (e.g. by the explosive charge used in the experiments [9]).
3) Passing of the crack opening profile from LS-DYNA to the fluid simulator.
4) The fluid simulator calculates the flow in the pipe and through the crack. The new pressure profile is applied to the pipeline structure.
5) The response of the pipeline structure is calculated as described in Section 2.
6) A new crack-opening profile, including possible erosion of new elements due to fracture, is calculated.

The time-step length in LS-DYNA is determined by the smallest element side of the structure and is typically around 10^{-6} s for the structure we have simulated here. The time-step length of the fluid calculations used to compute the 1D pressure profile depends on the flow according to a CFL-number

condition. The crack width $2r_e(x)$ as seen by the fluid code is never allowed to be larger than the initial pipe diameter.

In this paper, a simplified approximation to a radial pressure variation on the opening pipe is implemented. Once the crack width is larger than one pipe diameter (*i.e.* $2r_e(x) > 0.261$ m), the pressure calculated for a given structure element by the fluid simulator is scaled by the scalar product of the unit radial vector of the element and the unit normal vector to the element (see Figure 2), according to (17). This is an *ad hoc* way of making the force applied go smoothly towards zero as an element is wrapped away from the pipe interior.

$$p \propto \begin{cases} \hat{r} \cdot \hat{n} & , \quad \hat{r} \cdot \hat{n} > 0 \\ 0 & , \quad \hat{r} \cdot \hat{n} < 0 \end{cases} \tag{17}$$

Figure 2: Illustration of the two vectors used to scale the force applied to a given structure element, according to (17).

The backfill condition of the pipe is in this paper represented by a rigid plane on which the pipeline rests under the force of gravity. That is, the kinetic energy of opening pipeline walls is dissipated simply through plastic deformation of the steel material. The running fracture is initiated by eroding the elements corresponding to a 30 cm long through-thickness notch in the axial direction in the centre of the pipeline.

5. Numerical simulations

The main purpose of this paper is to show the difference in the fluid dynamics and the crack arrest properties of a pipeline pressurized with natural gas (methane) and pure CO_2. The boundary conditions for the simulations presented here are somewhat different than the experimental data available from the natural gas burst tests in [9]. In addition to this, experimental data for CO_2 burst tests are not available for comparison at the time of writing. For these reasons, a direct comparison with experimental results will not be presented in this paper. A pipeline pressurized with pure CO_2 or methane at 75, 120 and 150 bar has been simulated. Initial temperatures of 300 and 293K have been investigated for the CO_2. For the methane simulations, the initial temperature was 300K. No heat transfer has been considered during the simulations. For the methane cases, the parameters employed in the EOS are given in Table 1.

Table 1. EOS parameter values used in the simulations of methane.

	$\gamma = c_p/c_v$	c_p (J kg^{-1} K^{-1})
Methane, 75 bar	1.4109	1552.7
Methane, 120 bar	1.6133	1114.1
Methane, 150 bar	1.8059	933.72

The total length of the pipeline is 11.5 m. Symmetry in the axial direction is assumed, thus only half of the total pipe length was simulated. The FE-mesh of the steel pipeline consists of 28980 Belytschko-Tsay shell elements with 5 through-thickness integration points, giving a characteristic element length of 12.5 mm. The crack is then driven by the internal pressure profile along a predefined crack path. As illustrated in Figure 3, this crack path is modelled as a predefined "seam" where the elements are allowed to fail. In

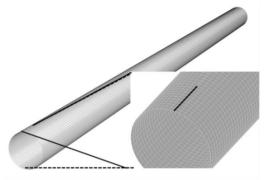the fluid simulator, a numerical grid of 383 cells and CFL numbers of 0.9 (methane) and 0.5 (CO_2) were employed.

Figure 3: Illustration of FE-mesh with predefined crack path (highlighted).
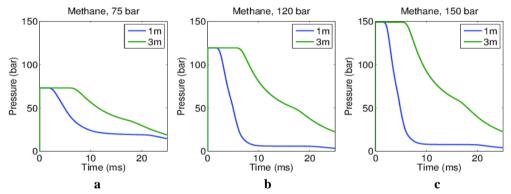

Figure 4: Pressure vs. time data at two positions for the methane cases at a) 75 bar, b) 120 bar and c) 150 bar initial pressure.
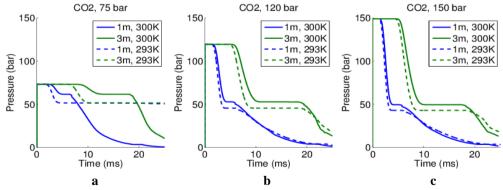

Figure 5: Pressure vs. time data at two positions for the CO_2 cases at a) 75 bar, b) 120 bar and c) 150 bar initial pressure.

Pressure at 1 and 3 m from the middle of the pipe in the axial direction are plotted as a function of time in Figure 4 and Figure 5 for the methane and CO_2 simulations, respectively. For both axial positions, pressure sensors were located at the 3 o'clock position. In Figure 6, the amount of fracture growth (excluding the length of the initial crack) is plotted as a function of time. As can be seen from Figure 6,

no crack arrest was observed in any of the CO_2 simulations at 300 K. In contrast, the methane simulations under the same conditions experienced crack arrest.
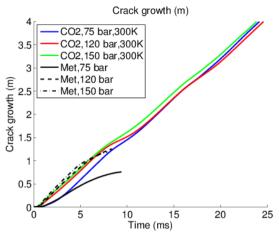

Figure 6: Crack growth in cases with CO_2 and methane cases.

From Figure 5 we clearly see the evidence of the CO_2 reaching its saturation pressure after the initial wave has passed. The second wave which decreases the pressure to a much lower value moves significantly slower than the initial wave. Our data indicate that the position of the crack tip follows the transition between the liquid and the liquid-vapour region. Thus, once the initial pressure wave has passed, the pressure at the crack tip is found to always be equal to the saturation pressure of the CO_2. This will be subject to further investigation. In any case, in the present simulations, the saturation pressure appears to be large enough to sustain the crack growth (except at 75 bar and 293K). In contrast, methane exhibits no such phase change and corresponding pressure plateau. This may explain the difference in crack-arrest prediction for the two gasses.

The present results are in qualitative agreement with those of Mahgerefteh *et al.* [19], who noted that CO_2 pipelines may be more susceptible to fracture propagation than hydrocarbon pipelines. Until data from full scale experiments are available for comparison and possible verification, these results indicate that based on the operating conditions of the CO_2 pipeline, the steel grade and dimensions must be selected carefully.

6. Conclusion

We believe that the present approach – to develop a coupled fluid-structure fracture assessment model – will contribute to an improved understanding of the interaction between the structural and the fluid dynamical behaviour. This, in turn, can enable a safe and cost-effective design and operation of CO_2 pipelines. For the initial pressure and temperature conditions studied here, our preliminary results indicate that when cracks are initiated in methane and CO_2 pipelines, the former may experience crack arrest while the latter might not. It was also indicated that the phase transition in CO_2 during depressurization is an important factor.

Future work may include the interaction between the crack propagation in the pipe and the phase transition in the CO_2, and more detailed studies of the flow through the crack, including the translation of fluid pressure into forces on structure elements. A better fundamental understanding of dynamic ductile crack growth and the main material factors determining the fracture velocity is also needed.

Acknowledgements

References

1. International Energy Agency (IEA). *Energy Technology Perspectives* 2012. ISBN 978-92-64-17488-7.

2. Maxey, W.A. Fracture initiation, propagation and arrest. In: *Fifth Symposium on Line Pipe Research*, American Gas Association, Houston, USA, 1974.

3. Makino, H., Inoue, T., Endo, S., Kubo, T. and Matsumoto, T. Simulation method for shear fracture propagation in natural gas transmission pipelines. In: *5th ISOPE Ocean mining Symposium*, Tsukuba, Japan, 2003, pp. 60–68.

4. Leis, B. N., Zhu, X-K., Forte, T.P. and Clark, E.B. Modeling running fracture in pipelines - past, present, and plausible future directions. In: *11th International conference on fracture,* Turin, Italy, 2005.

5. Titarev, V.A. and Toro, E.F. MUSTA schemes for multi-dimensional hyperbolic systems: analysis and improvements. *Int. J. Numer. Meth. Fluids* 2005;**49**:117–147.

6. Toro, E. F. MUSTA: A multi-stage numerical flux. *Appl. Numer. Math.* 2006;**56**:1464–1479.

7. Hallquist, J.O., LS-DYNA Keyword User's Manual, Livermore Software Technology Corporation. 2007.

8. Berstad, T., Dørum, C., Jakobsen, J.P., Kragset, S., Li, H., Lund, H., Morin, A., Munkejord, S.T., Mølnvik, M.J., Nordhagen, H.O. and Østby, E. CO_2 pipeline integrity: A new evaluation methodology, *Energy Procedia* 2011;**4**,:3000–3007.

9. Nordhagen, H.O., Kragset, S., Berstad, T., Morin, A., Dørum, C. and Munkejord, S.T. A new coupled fluid-structure modelling methodology for running ductile fracture. *Comput. Struct.* 2012;**94–95**:1006–1014.

10. Span, R. and Wagner, W.A. A new equation of state for carbon dioxide covering the fluid region from the triple-point temperature to 1100 K at pressures up to 800 MPa. *J. Phys. Chem. Ref. Data* 1996;**25**:1509–1596.

11. Besson, J., Luu, T.T., Tanguy, B. and Pineau, A. Anisotropic plastic and damage behavior of a high strength pipeline steel. In: *International Offshore and Polar Engineering Conference*, 2009.

12. Tanguy, B., Luu, T.T., Perrin, G., Pineau, A. and Besson, J. Plastic and damage behaviour of a high strength X100 pipeline steel: Experiments and modelling. *Int. J. Pres. Ves. Pip.* 2008;**85**:322–335.

13. Parks, D. M. and Freund, L. B. On the Gasdynamics of Running Ductile Fracture in a Pressurized Line Pipe, *J. Press. Vess. Technol.* 1978;**100**:13-17.

14. Ives, K. D., Shoemaker, A. and McCartney, R. Pipe Deformation During a Running Shear Fracture in Line Pipe. *J. Eng. Mater. Tech* 1974;**96**:309-317.

15. Giljarhus, K.E.T., Munkejord, S.T. and Skaugen, G. Solution of the Span–Wagner equation of state using a density-energy state function for fluid-dynamic simulation of carbon dioxide. *Ind. Eng. Chem. Res.* 2012;**51**:1006–1014.

16. Munkejord S.T., Evje S. and Flåtten T. The multi-stage centred-scheme approach applied to a drift-flux two-phase flow model. *Int. J. Numer. Meth. Fluids* 2006; **52**:679–705.

17. Munkejord S.T., Jakobsen J.P., Austegard A. and Mølnvik M.J. Thermo- and fluid-dynamical modelling of two-phase multi-component carbon dioxide mixtures. *Int. J. Greenh. Gas Con.* 2010;**4**:589–596.

18. Munkejord S.T., Evje S. and Flåtten T. A MUSTA scheme for a nonconservative two-fluid model. *SIAM J. Sci. Comp.* 2009; **31**:2587–2622.

19. Mahgerefteh, H., Brown, S. and Denton, G. Modelling the impact of stream impurities on ductile fractures in CO_2 pipelines. *Chem. Eng. Sci.* 2012;**74**:200–210.